

Adaptive numerical designs for the calibration of computer codes

Guillaume Damblin

EDF R&D MRI, Chatou, France
AgroParisTech / UMR INRA MIA
INRA, UMR 518, F-75005 Paris, France

Pierre Barbillon^{*†}

AgroParisTech / UMR INRA MIA
INRA, UMR 518, F-75005 Paris, France

Merlin Keller

EDF R&D MRI, Chatou, France

Alberto Pasanisi

EDF R&D MRI, Chatou, France
EIFER, Karlsruhe, Germany

Éric Parent

AgroParisTech / UMR INRA MIA
INRA, UMR 518, F-75005 Paris, France

September 1, 2022

Abstract

Making good predictions of a physical system using a computer code requires the inputs to be carefully specified. Some of these inputs called control variables have to reproduce physical conditions whereas other inputs, called parameters, are specific to the computer code and most often uncertain. The goal of statistical calibration consists in estimating these parameters with the help of a statistical model which links the code outputs with the field measurements. In a Bayesian setting, the posterior distribution of these parameters is normally sampled using MCMC methods. However, they are impractical when the code runs are high time-consuming. A way to circumvent this issue consists of replacing the computer code with a Gaussian process emulator, then sampling a cheap-to-evaluate posterior distribution based on it. Doing so, calibration is subject to an error which strongly depends on the numerical design of experiments used to fit the emulator. We aim at reducing this error by building a proper sequential design by means of the Expected Improvement criterion. Numerical illustrations in several dimensions assess the efficiency of such sequential strategies.

Keywords: Bayesian calibration, Gaussian process emulator, Expected Improvement criterion.

1 Introduction

This work is incorporated within the field of uncertainty quantification in computer experiments. A crucial issue in engineering (aerospace, car, nuclear, etc.) concerns the ability of computer codes (also called simulators or computer models) to mimic a physical phenomenon of interest

^{*}Corresponding author: 16 rue Claude Bernard, 75005 Paris

[†]PIERRE.BARBILLON@AGROPARISTECH.FR

as well as possible. In this regard, the field of so-called Verification and Validation (V&V) aims at assessing the accuracy of computer predictions for many applications. For instance, the study of V&V has become a huge preoccupation in the nuclear industry where numerical simulation is more and more used to assess the safety of installations for which physical experiments are impractical or economically infeasible. An essential prerequisite of V&V consists in quantifying all sources of uncertainty involved in a code output (Roy and Oberkampf, 2011). Our paper is focused on the reduction of one of them, called parameter uncertainty, caused by the lack of knowledge about the value of parameters which are specific to the computer code (Kennedy and O’Hagan, 2001). They can be either non-measurable physical quantities or just tuning factors. Calibration comes down to a statistical inference of these parameters after assuming a statistical model which makes explicit the relationship between the code outputs and the field measurements (Campbell, 2006; Cox et al., 2001). Another popular framework which deals with parameter uncertainty is called History Matching (HM) (Craig et al., 1997). HM aims at detecting regions of parameter space which appear to be incompatible with the field measurements. Based on an implausibility measure, this method is well-suited for large systems for which the size of inputs makes immediate calibration intractable. In the same way, Sensitivity Analysis (SA) aims at detecting which parameters have a negligible effect on the code output (Saltelli et al., 2000). Hence, both HM and SA can shrink the input space before carrying out calibration.

Our work focuses on calibration in a Bayesian fashion (Kennedy and O’Hagan, 2001; Bayarri et al., 2007), rather than frequentist methods (Loeppky et al., 2006; Gramacy et al., 2014; Wong et al., 2014). This strategy of inference provides an appropriate framework to quantify the parameter uncertainty from prior to posterior distribution as new data become available. In the literature, Bayesian calibration is performed within a framework where the code predictions suffer from a systematic discrepancy for any value of parameters, which reflects the view that the mathematical equations underlying the code should be not considered as a perfect modeling of the real world (Kennedy and O’Hagan, 2001; Higdon et al., 2004). Even if this framework is more realistic, some confounding can appear when the parameters and the shape of the discrepancy are jointly estimated (Loeppky et al., 2006; Brynjarsdottir and O’Hagan, 2014). Because this issue is not related with the scope of this paper, our presentation is centered on a statistical model which does not include the code discrepancy. However, it will be possible to generalize our framework provided the shape of the discrepancy is provided by prior expertise.

We aim at addressing Bayesian calibration when the code runs are time-consuming, which is a critical issue frequently arising in the field of computer experiments. Indeed, as simulations needs several hours, even several days to run, at that time the MCMC algorithms become burdensome. For instance, if each simulation lasts one hour, then 10000 simulations launched by an MCMC exploration of the parameter space will require more than a year, making the calibration process impractical. A well-known solution to this issue is to replace the code in the likelihood expression by a Gaussian process emulator (GPE) which is constructed from a training set of simulations run over a set of input locations, the so-called design of experiments. This paper propose two new algorithms for building sequential designs aiming at reducing the calibration error induced by the uncertainty of the GPE. Although it was already mentioned by Kennedy and O’Hagan (2001) as an important research axis, few papers deal with that issue. To the best of our knowledge, Kumar (2008) has already proposed some empirical criteria for sequentially selecting the code runs. Pratola et al. (2013) have also proposed some adaptive strategies whereby the Expected Improvement (EI) criterion is computed over a likelihood ratio. The EI criterion is used to optimize black box functions when a limited number of simulations is allocated (Jones et al., 1998). Recently, it has been applied to solving a problem of optimization

under uncertainty when the code inputs are (\mathbf{x}, \mathbf{u}) where \mathbf{x} denotes a vector of control variables and \mathbf{u} denotes a vector of random variables (Janusevskis and Le Riche, 2013). In the same spirit, we propose new algorithms which consist in applying the EI criterion to the sum of squares of the residuals between the code outputs and the field measurements when the code inputs are $(\mathbf{x}, \boldsymbol{\tau})$ where $\boldsymbol{\tau}$ is a vector of parameters. In this way, we aim at reducing the uncertainty due to the GPE in regions of high posterior density.

This paper is divided into five sections. In Section 2, the statistical framework is introduced, then the main features of the GPE are recalled. In Section 3, two new algorithms for Bayesian calibration based on the Expected Improvement criterion are presented. Their performances are illustrated on two academic examples in Section 4. The conclusions of this paper are provided in Section 5.

2 Calibration framework

Notations and modeling Let $r(\mathbf{x}) \in \mathbb{R}$ be a physical quantity of interest where $\mathbf{x} = (x^1, \dots, x^d) \in \mathcal{X} \subset \mathbb{R}^d$ is a vector of control variables. This kind of variable is measurable in the field experiments and characterizes the system. It can include both physical variables (temperature, pressure, velocity, etc.) and design variables (height, area, etc.). We suppose that a number of field experiments, say n , has been collected. In this paper, the sites of field experiments will refer to as the matrix $\mathbf{X}_f = [(\mathbf{x}_f^1)^T, \dots, (\mathbf{x}_f^n)^T]^T \in M_{n,d}(\mathbb{R})$ and the corresponding measurements will refer to as the vector $\mathbf{z}_f = (z_f^1, \dots, z_f^n)^T$. Due mainly to the measurements errors, \mathbf{z}_f is not exactly equal to $r(\mathbf{X}_f) = (r(\mathbf{x}_f^1), \dots, r(\mathbf{x}_f^n))$. Hence, for $1 \leq i \leq n$,

$$z_f^i = r(\mathbf{x}_f^i) + \epsilon^i, \quad (1)$$

where

$$\epsilon^i \underset{i.i.d.}{\sim} \mathcal{N}(0, \lambda^2), \quad (2)$$

is modeled as a white noise. The variance λ^2 is assumed to be known because in many cases, either the precision of the measuring device is known or it can be estimated from replicates.

Let $y_{\boldsymbol{\tau}}(\mathbf{x})$ be a deterministic computer code which predicts $r(\mathbf{x})$ where $\boldsymbol{\tau} \in \mathcal{T} \subset \mathbb{R}^m$ is a vector of parameters including either factors attached to the field (chemical rate, friction coefficient, etc.) or mathematical tuning factors such as a discretization step having no counterpart in physics, or perhaps both (Gang et al., 2009). The computer code is seen as a black box function, which supposes nothing is known about the connection between the inputs $(\mathbf{x}, \boldsymbol{\tau})$ and the output $y_{\boldsymbol{\tau}}(\mathbf{x})$. A simulation refers to a code output $y_{\boldsymbol{\tau}}(\mathbf{x})$. A numerical design of experiments means a set of input locations from which the code is run (Koehler and Owen, 1996). Following Kennedy and O'Hagan (2001), the computer code should be considered as an imperfect representation of the phenomenon r . Hence,

$$r(\mathbf{x}) = y_{\boldsymbol{\theta}}(\mathbf{x}) + b(\mathbf{x}), \quad (3)$$

where $b(\mathbf{x})$ is the code discrepancy and $\boldsymbol{\theta}$ is the optimal value of parameters. Combining (3) and (1), the statistical model which links the simulations with the field measurements is written as

$$z_f^i = y_{\boldsymbol{\theta}}(\mathbf{x}_f^i) + b(\mathbf{x}_f^i) + \epsilon^i. \quad (4)$$

The computer code is said to be calibrated when an estimator $\hat{\boldsymbol{\theta}}$ of $\boldsymbol{\theta}$ has been calculated as being the “best-fitting” parameter according to the statistical model (4). Due to potential non-identifiability between $\boldsymbol{\theta}$ and $b(\mathbf{x})$ in this model, the estimation of $\boldsymbol{\theta}$ requires to set some

prior hypothesis on the shape of $b(\mathbf{x})$. This issue has been widely studied over the past decade. Kennedy and O'Hagan (2001), Higdon et al. (2004) and many others have modeled $b(\mathbf{x})$ by a Gaussian process. Joseph and Melkote (2009) have proposed to use a more common regression model instead.

In our statistical setting, we suppose that $b(\mathbf{x})$ is negligible in the sense where it can not be distinguished from the noise ϵ . If $b(\mathbf{x})$ is significant, then the method developed in this paper could be still applied if it has been elicited from prior expertise.

The unbiased model Let us suppose that $b(\mathbf{x}) = 0$. In other words, for at least one value in \mathcal{T} denoted by $\boldsymbol{\theta}$, the computer code is supposed to be a perfect representation of the physical phenomenon r , which means that

$$\exists \boldsymbol{\theta} \in \mathcal{T} ; \forall \mathbf{x} \in \mathcal{X}, r(\mathbf{x}) = y_{\boldsymbol{\theta}}(\mathbf{x}). \quad (5)$$

Combining (5) and (1) leads to the equation

$$z_f^i = y_{\boldsymbol{\theta}}(\mathbf{x}_f^i) + \epsilon^i. \quad (6)$$

We have chosen to conduct a Bayesian inference of $\boldsymbol{\theta}$ because it has been shown better suited than the standard MLE¹, where flat likelihood may need regularization, especially if the dimension of $\boldsymbol{\theta}$ is high (Kumar, 2008). Let $y_{\boldsymbol{\theta}}(\mathbf{X}_f) := (y_{\boldsymbol{\theta}}(\mathbf{x}_f^1), \dots, y_{\boldsymbol{\theta}}(\mathbf{x}_f^n))^T$ be the vector of code outputs running over the input field data \mathbf{X}_f . The posterior distribution of $\boldsymbol{\theta}$ given by the Bayes formula is a normalized version of the following product:

$$\begin{aligned} \Pi(\boldsymbol{\theta}|\mathbf{z}_f) &\propto \mathcal{L}(\mathbf{z}_f|\boldsymbol{\theta})\Pi(\boldsymbol{\theta}), \\ &\propto \frac{1}{(\sqrt{2\pi}\lambda)^n} \exp \left[-\frac{1}{2\lambda^2} SS(\boldsymbol{\theta}) \right] \Pi(\boldsymbol{\theta}), \end{aligned} \quad (7)$$

where

$$SS(\boldsymbol{\theta}) = \|\mathbf{z}_f - y_{\boldsymbol{\theta}}(\mathbf{X}_f)\|^2 \quad (8)$$

is the sum of squares of the residuals between the simulations $y_{\boldsymbol{\theta}}(\mathbf{X}_f)$ and the field measurements. Throughout this paper, $\Pi(\boldsymbol{\theta}|\mathbf{z}_f)$ is referred to as the target posterior distribution. No closed-form expression exists for $\Pi(\boldsymbol{\theta}|\mathbf{z}_f)$ because y is usually highly non linear with respect to $\boldsymbol{\theta}$. In such cases, $\Pi(\boldsymbol{\theta}|\mathbf{z}_f)$ needs to be sampled by running an MCMC algorithm which converges to $\Pi(\boldsymbol{\theta}|\mathbf{z}_f)$ over a very large number of samples, often several thousand (Robert and Casella, 1998). In our framework, the MCMC algorithms are thus impractical since each sample requires a time-consuming simulation. A way to circumvent this issue consists in setting a Gaussian Process Emulator (GPE), denoted by $Y(\cdot)$, as a prior distribution on $y(\cdot)$ where (\cdot) corresponds to a pair of inputs $(\mathbf{x}, \boldsymbol{\tau})$. In the following, we need to employ the notation $\boldsymbol{\tau} \in \mathcal{T}$ which refers to any value of the code parameter whereas $\boldsymbol{\tau} = \boldsymbol{\theta}$ refers to the optimal value to be estimated.

Gaussian process emulator The Gaussian process was first developed within the field of computer experiments by Sacks et al. (1989). It is the most familiar surrogate model used to mimic a costly computer code. From a Bayesian perspective, the Gaussian process, denoted in this paper by $Y(\cdot)$, should be considered as a prior structure on the code (Currin et al., 1991):

$$Y(\cdot) \sim \mathcal{GP}(m_{\beta}(\cdot), \sigma^2 C_{\Psi}(\cdot, \cdot)), \quad (9)$$

where

¹Maximum Likelihood Estimation

- $m_{\boldsymbol{\beta}}(\cdot) = h(\cdot)^T \boldsymbol{\beta}$ where $h(\cdot) = (h_1(\cdot), \dots, h_p(\cdot))^T$ is a vector of regression functions and $\boldsymbol{\beta} \in \mathbb{R}^p$ is a vector of location parameters,
- σ^2 the variance of the process,
- $C_{\boldsymbol{\Psi}}(\cdot, \cdot)$ is the correlation function where $\boldsymbol{\Psi}$ is a vector of hyper-parameters including a range parameter and possibly a smoothness parameter.

The choice of the correlation function $C_{\boldsymbol{\Psi}}(\cdot, \cdot)$ should depend on the prior information about the shape of the code output over $\mathcal{X} \times \mathcal{T}$. In addition, for both practical and theoretical reasons, a stationary function is almost always specified (Stein, 1999). Let $\mathbf{D}_N \in (\mathcal{X} \times \mathcal{T})^N$ be a numerical design of experiments:

$$\mathbf{D}_N := \{(\mathbf{x}^1, \boldsymbol{\tau}^1), \dots, (\mathbf{x}^N, \boldsymbol{\tau}^N)\}. \quad (10)$$

After running the code over \mathbf{D}_N , N simulations can be collected:

$$y(\mathbf{D}_N) := \left(y(\mathbf{x}^1, \boldsymbol{\tau}^1) := y_{\boldsymbol{\tau}^1}(\mathbf{x}^1), \dots, y(\mathbf{x}^N, \boldsymbol{\tau}^N) := y_{\boldsymbol{\tau}^N}(\mathbf{x}^N) \right)^T. \quad (11)$$

Let \mathbf{v}_{pred} and \mathbf{v}'_{pred} be two vectors in $\mathcal{X} \times \mathcal{T}$. Then,

- $\Sigma_{\boldsymbol{\Psi}}(\mathbf{D}_N) = C_{\boldsymbol{\Psi}}((\mathbf{x}^i, \boldsymbol{\tau}^i), (\mathbf{x}^j, \boldsymbol{\tau}^j))_{1 \leq i, j \leq N}$ is the matrix of correlations between the simulations $y(\mathbf{D}_N)$,
- $\Sigma_{\boldsymbol{\Psi}}(\mathbf{v}_{pred}, \mathbf{D}_N) = (C_{\boldsymbol{\Psi}}(\mathbf{v}_{pred}, (\mathbf{x}^i, \boldsymbol{\tau}^i)))_{1 \leq i \leq N}$ is the vector of correlations between $Y(\mathbf{v}_{pred})$ and each of $y(\mathbf{D}_N)$.

By conditioning the Gaussian process (9) on the training set of simulations $y(\mathbf{D}_N)$, the resulting process is still a Gaussian process:

$$Y^N(\cdot) := Y(\cdot) | y(\mathbf{D}_N) \sim \mathcal{GP}(\mu_{\boldsymbol{\beta}}^N(\cdot), V_{\boldsymbol{\Psi}, \sigma^2}^N(\cdot, \cdot)), \quad (12)$$

with the standard expressions for the conditional mean and covariance:

$$\begin{aligned} \mu_{\boldsymbol{\beta}, \boldsymbol{\Psi}}^N(\mathbf{v}_{pred}) &= \mathbb{E}[Y^N(\mathbf{v}_{pred})] \\ &= m_{\boldsymbol{\beta}}(\mathbf{v}_{pred}) + \Sigma_{\boldsymbol{\Psi}}(\mathbf{v}_{pred}, \mathbf{D}_N)^T \Sigma_{\boldsymbol{\Psi}}(\mathbf{D}_N)^{-1} [y(\mathbf{D}_N) - m_{\boldsymbol{\beta}}(\mathbf{v}_{pred})], \end{aligned} \quad (13)$$

and

$$\begin{aligned} V_{\boldsymbol{\Psi}, \sigma^2}^N(\mathbf{v}_{pred}, \mathbf{v}'_{pred}) &= \text{Cov}(Y^N(\mathbf{v}_{pred}), Y^N(\mathbf{v}'_{pred})) \\ &= \sigma^2 \left(C_{\boldsymbol{\Psi}}(\mathbf{v}_{pred}, \mathbf{v}'_{pred}) - \Sigma_{\boldsymbol{\Psi}}(\mathbf{v}_{pred}, \mathbf{D}_N)^T \Sigma_{\boldsymbol{\Psi}}(\mathbf{D}_N)^{-1} \Sigma_{\boldsymbol{\Psi}}(\mathbf{v}'_{pred}, \mathbf{D}_N) \right). \end{aligned} \quad (14)$$

The GPE is given by the conditional process (12) which yields a stochastic prediction of the code for any input \mathbf{v}_{pred} of the input space $\mathcal{X} \times \mathcal{T}$. In the case where \mathbf{v}_{pred} belongs to \mathbf{D}_N , the GPE interpolates the simulations $y(\mathbf{D}_N)$, that is for $1 \leq i \leq N$

$$\mu_{\boldsymbol{\beta}}^N(\mathbf{x}^i, \boldsymbol{\tau}^i) = y(\mathbf{x}^i, \boldsymbol{\tau}^i),$$

and

$$V_{\boldsymbol{\Psi}, \sigma^2}^N((\mathbf{x}^i, \boldsymbol{\tau}^i), (\mathbf{x}^i, \boldsymbol{\tau}^i)) = 0$$

which is expected for such an emulator of a deterministic computer code. Lastly, the capability of a GPE to predict well the code should be checked thanks to some validation criteria (Bastos and O'Hagan, 2008). For more details about the GPE, refer to Rasmussen and Williams (2006), Santner et al. (2003), Fang et al. (2006). Other more theoretical references dedicated to asymptotic properties are Stein (1999) and Bachoc (2014).

Calibration using a GPE In Equation (8), the simulations $y_{\boldsymbol{\theta}}(\mathbf{X}_f)$ are replaced with a GPE constructed from a design of experiments \mathbf{D}_N . Let,

- $m_{\boldsymbol{\beta}}(\mathbf{D}_N) = (h(\mathbf{x}^1, \boldsymbol{\tau}^1)^T \boldsymbol{\beta}, \dots, h(\mathbf{x}^N, \boldsymbol{\tau}^N)^T \boldsymbol{\beta})^T$ be the mean vector of the Gaussian process evaluated in each location of \mathbf{D}_N ,
- $m_{\boldsymbol{\beta}}(\mathbf{X}_f, \boldsymbol{\theta})$ and $\Sigma_{\Psi}(\mathbf{X}_f, \boldsymbol{\theta})$ be the mean vector and the correlation matrix of the Gaussian process, each evaluated in $(\mathbf{X}_f, \boldsymbol{\theta}) := ((\mathbf{x}_f^1, \boldsymbol{\theta}), \dots, (\mathbf{x}_f^n, \boldsymbol{\theta}))^T$,
- $\Sigma_{\Psi}(\mathbf{D}_N, (\mathbf{X}_f, \boldsymbol{\theta}))$ be the correlation matrix between \mathbf{D}_N and $(\mathbf{X}_f, \boldsymbol{\theta})$.

Then, we now consider the available data $\mathbf{d} := (y(\mathbf{D}_N), \mathbf{z}_f)$. The joint likelihood of $\boldsymbol{\theta}$ and $(\boldsymbol{\beta}, \sigma^2, \Psi)$ is given by

$$\mathcal{L}^F(\mathbf{d}|\boldsymbol{\theta}, \sigma^2, \boldsymbol{\beta}, \Psi) \propto \frac{|C_{\Psi}|^{-1/2}}{\sigma^{N+n}} \exp -\frac{1}{2\sigma^2} \left[(\mathbf{d} - (m_{\boldsymbol{\beta}}(\mathbf{D}_N), m_{\boldsymbol{\beta}}(\mathbf{X}_f, \boldsymbol{\theta})))^T C_{\Psi}^{-1} (\mathbf{d} - (m_{\boldsymbol{\beta}}(\mathbf{D}_N), m_{\boldsymbol{\beta}}(\mathbf{X}_f, \boldsymbol{\theta}))) \right], \quad (15)$$

where

$$C_{\Psi} = \begin{pmatrix} \Sigma_{\Psi}(\mathbf{D}_N) & \Sigma_{\Psi}(\mathbf{D}_N, (\mathbf{X}_f, \boldsymbol{\theta})) \\ \Sigma_{\Psi}(\mathbf{D}_N, (\mathbf{X}_f, \boldsymbol{\theta}))^T & \Sigma_{\Psi}(\mathbf{X}_f, \boldsymbol{\theta}) + \frac{\lambda^2}{\sigma^2} \mathbf{I}_n \end{pmatrix}.$$

In the previous paragraph about the GPE, the parameters $\boldsymbol{\beta}$, σ^2 and Ψ have been assumed to be known. If they are not, their estimation should be conducted jointly with $\boldsymbol{\theta}$ based on the full likelihood (15) (Higdon et al., 2004). However, inspired from the pioneering work of Cox et al. (2001), a two-step procedure can be conducted instead. This technique, known as modularization in Liu et al. (2009), is still used in a recent work dealing with calibration (Gramacy et al., 2014). It first consists in estimating the parameters $\boldsymbol{\beta}$, σ^2 and Ψ only thanks to the simulations $y(\mathbf{D}_N)$ by maximizing the marginal density of $y(\mathbf{D}_N)$, denoted by \mathcal{L}^M :

$$\mathcal{L}^M(y(\mathbf{D}_N)|\sigma^2, \boldsymbol{\beta}, \Psi) \propto \frac{|\Sigma_{\Psi}(\mathbf{D}_N)|^{-1/2}}{\sigma^N} \exp \left\{ -\frac{1}{2\sigma^2} \left[(y(\mathbf{D}_N) - m_{\boldsymbol{\beta}}(\mathbf{D}_N))^T \Sigma_{\Psi}(\mathbf{D}_N)^{-1} (y(\mathbf{D}_N) - m_{\boldsymbol{\beta}}(\mathbf{D}_N)) \right] \right\}, \quad (16)$$

Then, the \mathcal{L}^M 's maximum likelihood estimates (MLEs) $(\hat{\sigma}^2, \hat{\boldsymbol{\beta}}, \hat{\Psi})$ of $(\sigma^2, \boldsymbol{\beta}, \Psi)$ are plugged into the likelihood of \mathbf{z}_f conditional to the simulations $y(\mathbf{D}_N)$, denoted below by \mathcal{L}^C :

$$\mathcal{L}^C(\mathbf{z}_f|\boldsymbol{\theta}, y(\mathbf{D}_N)) \propto |V_{\hat{\Psi}, \hat{\sigma}^2}^N(\boldsymbol{\theta}) + \lambda^2 \mathbf{I}_n|^{-1/2} \exp \left\{ -\frac{1}{2} \left[(\mathbf{z}_f - \mu_{\hat{\boldsymbol{\beta}}, \hat{\Psi}}^N(\mathbf{X}_f, \boldsymbol{\theta}))^T (V_{\hat{\Psi}, \hat{\sigma}^2}^N(\boldsymbol{\theta}) + \lambda^2 \mathbf{I}_n)^{-1} (\mathbf{z}_f - \mu_{\hat{\boldsymbol{\beta}}, \hat{\Psi}}^N(\mathbf{X}_f, \boldsymbol{\theta})) \right] \right\} \quad (17)$$

where

$$\mu_{\hat{\boldsymbol{\beta}}, \hat{\Psi}}^N(\mathbf{X}_f, \boldsymbol{\theta}) := (\mu_{\hat{\boldsymbol{\beta}}, \hat{\Psi}}(\mathbf{x}_f^1, \boldsymbol{\theta}), \dots, \mu_{\hat{\boldsymbol{\beta}}, \hat{\Psi}}(\mathbf{x}_f^n, \boldsymbol{\theta}))^T,$$

and

$$V_{\hat{\Psi}, \hat{\sigma}^2}^N(\boldsymbol{\theta})(i, j) = \text{Cov}(Y^N(\mathbf{x}_f^i, \boldsymbol{\theta}), Y^N(\mathbf{x}_f^j, \boldsymbol{\theta})).$$

This modular approach goes hand-in-hand with intuition whereby the estimation of the calibration parameter $\boldsymbol{\theta}$ should be separated from the estimation of σ^2 , $\boldsymbol{\beta}$ and $\boldsymbol{\Psi}$ because they are of different natures. Kennedy and O’Hagan (2001) also argue it is not a great loss to estimate σ^2 , $\boldsymbol{\beta}$ and $\boldsymbol{\Psi}$ only thanks to $y(\mathbf{D}_N)$ because the number of field measurements n is usually much smaller than N . Liu et al. (2009) has put in light a poorer mixing in the MCMC routine based on the full likelihood (15) than based on (17). From now on, the conditional likelihood (17) is referred to as the approximated likelihood. Let Π^C denote the approximated posterior distribution induced by (17). Then,

$$\Pi^C(\boldsymbol{\theta}|\mathbf{z}_f, y(\mathbf{D}_N)) \propto \mathcal{L}^C(\mathbf{z}_f|\boldsymbol{\theta}, y(\mathbf{D}_N))\Pi(\boldsymbol{\theta}). \quad (18)$$

The approximated posterior (18) and the target posterior (7) are different in that $y_{\boldsymbol{\theta}}(\mathbf{X}_f)$ is replaced by the mean vector of the GPE $\mu_{\boldsymbol{\beta}}^N(\mathbf{X}_f, \boldsymbol{\theta})$ and the conditional covariance matrix $V_{\boldsymbol{\Psi}, \sigma^2}^N(\boldsymbol{\theta})$ is added up to $\lambda^2 \mathbf{I}_n$. Contrary to the target posterior (7), the approximated posterior is cheap to evaluate, enabling to perform an MCMC algorithm in order to estimate $\boldsymbol{\theta}$.

Remark 1. The first stage of the modular approach neglects the uncertainty of the parameters σ^2 , $\boldsymbol{\beta}$ and $\boldsymbol{\Psi}$ by fixing them to their MLE. However, a possible manner to take in account their uncertainty would consist in adopting a Bayesian inference of σ^2 , $\boldsymbol{\beta}$ and $\boldsymbol{\Psi}$ in the same way than $\boldsymbol{\theta}$. For instance, if a Jeffreys prior distribution is specified on $(\boldsymbol{\beta}, \sigma^2)$, then the distribution of the GPE follows a Student distribution (Santner et al., 2003). Yet unfortunately, the conditional likelihood (17) has no closed-form expression anymore, causing an additional issue which is not the core of this paper.

In presence of a code discrepancy $b(\mathbf{x})$ The calibration setting (7) has to be modified to prevent overfitting of $\boldsymbol{\theta}$, as showed in Bayarri et al. (2007). In Higdon et al. (2004) and Bayarri et al. (2007), $b(\mathbf{x})$ is modeled by a zero mean Gaussian process

$$b(\cdot) \sim \mathcal{GP}(0, \sigma_b^2 C_{\boldsymbol{\Psi}_b}(\cdot, \cdot))$$

where (\cdot) corresponds here to an input \mathbf{x} . In this case, the logarithm of the approximated likelihood (17) is now proportional to a weighted sum of squares of the residuals:

$$SS(\boldsymbol{\theta}) = (\mathbf{z}_f - y_{\boldsymbol{\theta}}(\mathbf{X}_f))^T (V_f^b + \lambda^2 \mathbf{I}_n)^{-1} (\mathbf{z}_f - y_{\boldsymbol{\theta}}(\mathbf{X}_f)) \quad (19)$$

where $V_f^b(i, j) = \sigma_b^2 C_{\boldsymbol{\Psi}_b}(\mathbf{x}_f^i, \mathbf{x}_f^j)$. Sometimes, physical context helps us to fixed both σ_b^2 and $\boldsymbol{\Psi}_b$ to plausible values, as done in Craig et al. (2001). In such cases, V_f^b becomes known and the algorithms that we present in Section 3 will be still practicable based on (19) instead of (8).

Main goal of the paper Our work focuses on reducing the distance between the approximated posterior distribution (18) and the target posterior distribution (7). The Kullback-Leibler (KL) divergence shows interesting theoretical properties to measure how far is a probability distribution from a reference one (Cover and Thomas, 2006). It is written as

$$\text{KL}(\Pi(\boldsymbol{\theta}|\mathbf{z}_f) || \Pi^C(\boldsymbol{\theta}|\mathbf{z}_f, y(\mathbf{D}_N))) = \int_{\boldsymbol{\theta}} \Pi(\boldsymbol{\theta}|\mathbf{z}_f) \left(\log(\Pi(\boldsymbol{\theta}|\mathbf{z}_f)) - \log(\Pi^C(\boldsymbol{\theta}|\mathbf{z}_f, y(\mathbf{D}_N))) \right) d\boldsymbol{\theta}. \quad (20)$$

The design of experiments \mathbf{D}_N By using results of approximation theory, we can prove the proposition below.

Proposition 1. Under the following assumptions:

- $\Pi(\boldsymbol{\theta})$ has a bounded support \mathcal{T} ,
- the code output $y_{\boldsymbol{\tau}}(\mathbf{x})$ is uniformly bounded on $\mathcal{T} \times \mathcal{X}$,
- the correlation function (kernel) is a classical radial basis function (Schaback, 1995),
- y lies in the associated Reproducing Kernel Hilbert Space,
- the covering distances associated with the sequence of designs $(\mathbf{D}_N)_N$ tends to 0 with $N \rightarrow \infty$ (see Appendix),

then, we have:

$$\lim_{N \rightarrow \infty} \text{KL}(\Pi(\boldsymbol{\theta}|\mathbf{z}_f) || \Pi^C(\boldsymbol{\theta}|\mathbf{z}_f, y(\mathbf{D}_N))) = 0. \quad (21)$$

Proof. (21) results from the uniform convergence of $|\log(\Pi(\boldsymbol{\theta}|\mathbf{z}_f)) - \log(\Pi^C(\boldsymbol{\theta}|\mathbf{z}_f, y(\mathbf{D}_N)))|$ to 0 over \mathcal{T} when N tends to ∞ (see Appendix). Then, we can exchange limit and integral in (20), which completes the proof. \square

This proposition reflects the fact that the calibration based on the approximated posterior (18) is consistent, in other words the larger \mathbf{D}_N the closer the approximated posterior (18) to the target posterior (7). However, when N is small according to the dimension of the input space $\mathcal{X} \times \mathcal{T}$, (18) can be significantly different from (7) leading to a large KL divergence (20). Although an approximate posterior distribution constructed from an accurate GPE is likely to yield a small value of the KL-divergence (20), our own experience has shown such behavior is not systematic.

In practical use, \mathbf{D}_N is built as a space-filling design on the input space $\mathcal{X} \times \mathcal{T}$ (Pronzato and Muller, 2012), and thus not taking into account that \mathbf{x} and $\boldsymbol{\tau}$ have different roles to play in calibration. In fact, our interest is not to predict well the computer code over $\mathcal{X} \times \mathcal{T}$ but rather to minimize the KL-divergence (20), which can be developed as

$$\begin{aligned} \text{KL}(\Pi(\boldsymbol{\theta}|\mathbf{z}_f) || \Pi^C(\boldsymbol{\theta}|\mathbf{z}_f, y(\mathbf{D}_N))) &= \int_{\boldsymbol{\theta}} \Pi(\boldsymbol{\theta}|\mathbf{z}_f) (C - C_N(\boldsymbol{\theta})) d\boldsymbol{\theta} + \frac{1}{2} \int_{\boldsymbol{\theta}} \Pi(\boldsymbol{\theta}|\mathbf{z}_f) \\ &\quad \left((\mathbf{z}_f - \mu_{\boldsymbol{\beta}}^N(\mathbf{X}_f, \boldsymbol{\theta}))^T (V_{\boldsymbol{\Psi}, \sigma^2}^N(\boldsymbol{\theta}) + \lambda^2 \mathbf{I}_n)^{-1} (\mathbf{z}_f - \mu_{\boldsymbol{\beta}}^N(\mathbf{X}_f, \boldsymbol{\theta})) - SS(\boldsymbol{\theta}) \right) d\boldsymbol{\theta} \end{aligned} \quad (22)$$

where

$$C = -\frac{n}{2} \log \lambda^2, \quad (23)$$

and

$$C_N(\boldsymbol{\theta}) = -\frac{1}{2} \log |V_{\boldsymbol{\Psi}, \sigma^2}^N(\boldsymbol{\theta}) + \lambda^2 \mathbf{I}_n|. \quad (24)$$

According to Equation (22), the KL-divergence could be minimized by reducing the uncertainty of the GPE over input locations in the subspace $\mathbf{X}_f \times \mathcal{T}^n \subset (\mathcal{X} \times \mathcal{T})^n$ and above all where the target posterior distribution $\Pi(\mathbf{z}_f|\boldsymbol{\theta})$ is high. In Section 3, we propose new algorithms for building proper numerical designs \mathbf{D}_N designed for this purpose.

3 Adaptive designs for calibration

To identify the global minimum of a costly black box code, denoted by f (to avoid confusion with the calibration setting), the most efficient strategies are based on the Expected Improvement (EI) criterion (Jones et al., 1998). They consist in identifying sequentially the input locations where the code f should be run to be close to the global minimum, which is relevant when only a small number of simulations is allocated. Assuming k simulations $f(\mathbf{D}_k)$ have already been run, the EI criterion assesses the expected improvement of a new run (numbered $k+1$) in terms of getting close to the unknown global minimum of f . Let \mathbf{v}_{k+1} be the input where the EI value is at its highest, meaning that,

$$\begin{aligned}\mathbf{v}_{k+1} &= \underset{\mathbf{v}}{\operatorname{argmax}} EI^k(\mathbf{v}), \\ &= \underset{\mathbf{v}}{\operatorname{argmax}} \mathbb{E}[(m_k - F^k(\mathbf{v})) \mathbf{1}_{F^k(\mathbf{v}) < m_k}],\end{aligned}\tag{25}$$

where

- $F^k(\mathbf{v})$ is the current GPE which is built from \mathbf{D}_k ,
- $m_k = \min \{f(\mathbf{v}_1), \dots, f(\mathbf{v}_{k-1}), f(\mathbf{v}_k)\}$ is the current value for the minimum.

If a deterministic emulator were used instead of $F^k(\mathbf{v})$, for instance the mean $\mu(\mathbf{v})$ of $F^k(\mathbf{v})$, the EI criterion would be just the difference $m_k - \mu(\mathbf{v})$ if $\mu(\mathbf{v}) < m_k$ and 0 if $\mu(\mathbf{v}) > m_k$. Given $F^k(\mathbf{v})$ is stochastic, Equation (25) is written as the expectation of this truncated difference with respect to the distribution of F^k . The algorithm that consists of running the code at the input \mathbf{v}_{k+1} then updating the emulator and starting again is called Efficient Global Optimization (EGO) (Jones et al., 1998). The convergence of the EGO algorithm to the global minimum of f has been proven with respect to some assumptions about both the smoothness of the code and the correlation function of the GPE (Vazquez and Bect, 2010). In current use, the algorithm is stopped when the number of allocated simulations is over or when the improvement of m_k becomes negligible. According to this last criterion, EGO requires less simulations than other optimization methods with comparable levels of performance (Ginsbourger, 2009).

EI designed for calibration Our contribution now consists in resorting to the EI criterion for the sum of squares of the residuals function $SS(\boldsymbol{\theta})$:

$$EI^k(\boldsymbol{\theta}) = \mathbb{E} \left[(m_k - SS^k(\boldsymbol{\theta})) \mathbf{1}_{SS^k(\boldsymbol{\theta}) \leq m_k} \right] \in [0, m_k],\tag{26}$$

where

- $m_k := \min \{SS(\boldsymbol{\theta}_1), \dots, SS(\boldsymbol{\theta}_{k-1}), SS(\boldsymbol{\theta}_k)\}$ and $SS(\cdot)$ denotes the sum of squares computed from actual runs of the computer code y ,
- $SS^k(\cdot)$ denotes the sum of squares of the residuals where y is replaced with the GPE conditional to $y(\mathbf{D}_k)$, denoted by

$$Y^k(\cdot) = Y(\cdot) | y(\mathbf{D}_k),$$

where the subscript k now refers to the current iteration of the algorithm. $SS^k(\cdot)$ is thus a random process and its distribution inherits from the current GPE. At step k , nk new simulations need to be run to update m_k . Hence, the design \mathbf{D}_k contains all the simulations $y_{\boldsymbol{\theta}_j}(\mathbf{x}_f^i)$ for all $1 \leq i \leq n$ and $1 \leq j \leq k$ (do not confound with the notation in Section 2 where N has referred to the number of simulations). Let $\boldsymbol{\theta}^*$ be the maximum of (26):

$$\boldsymbol{\theta}^* = \underset{\boldsymbol{\theta}}{\operatorname{argmax}} EI^k(\boldsymbol{\theta}).$$

Justification for minimizing $SS(\theta)$ As explained at the end of the previous section, running the code over input locations in $\mathbf{X}_f \times \mathcal{T}$ where $\Pi(\mathbf{z}_f|\theta)$ is high reduces the distance between $\Pi^C(\mathbf{z}_f|\theta, y(\mathbf{D}_N))$ and $\Pi(\mathbf{z}_f|\theta)$. In addition, when no expert knowledge is available on the value of θ (except perhaps a lower and an upper bound), a noninformative prior should be specified for θ (Kass and Wasserman, 1996; Box and Tiao, 1973). In such cases, the higher the target posterior distribution $\Pi(\mathbf{z}_f|\theta)$, the lower $SS(\theta)$. The KL-divergence (20) can be then reduced faster by running the code over the input locations $(\mathbf{x}_f^i, \theta^*) \in \mathbf{X}_f \times \mathcal{T}$ where $SS(\theta^*)$ is small. Such locations θ^* can be identified by maximizing the EI criterion.

Remark 2. In some works, calibration consists in minimizing a gap between the code outputs and the available field measurements, such as $SS(\theta)$ (Wong et al., 2014) or a weighted sum of squares like (19) (Joseph and Melkote, 2009). For our part, the EI criterion applied to $SS(\theta)$ is just a circuitous way to efficiently build \mathbf{D}_N for Bayesian calibration.

EGO algorithms Algorithm 1 corresponds to an exact EGO algorithm based on Equation (26). It aims at identifying the input locations $(\mathbf{x}_f^i, \theta^*) \in \mathbf{X}_f \times \mathcal{T}$ which will be added up sequentially to an initial design \mathbf{D}_0 for N iterations. Algorithm 2 is a one at time algorithm and should be understood as an approximation of Algorithm 1.

Algorithm 1

Initialization

- Build a maximin Latin Hypercube Design (LHD) $\mathbf{D}_0 \subset \mathcal{X} \times \mathcal{T}$ of size N_0 .
- Run the code over \mathbf{D}_0 .
- Compute $\hat{\theta}_1$ as the maximum of $\Pi^C(\theta|\mathbf{z}_f, \mathbf{D}_0)$.
- $\mathbf{D}_1 = \mathbf{D}_0 \cup \{(\mathbf{x}_f^i, \hat{\theta}_1)\}_{1 \leq i \leq n}$.
- Update the Gaussian process distribution after running the code over $\{(\mathbf{x}_f^i, \hat{\theta}_1)\}_{1 \leq i \leq n}$.
- Set $m_1 := SS(\hat{\theta}_1)$.

From $k = 1$, repeat the following steps as long as $N_0 + n \times (k + 1) \leq N$.

Step 1 Find an estimate $\hat{\theta}_{k+1}$ of $\theta_{k+1}^* = \underset{\theta}{\operatorname{argmax}} EI^k(\theta)$.

Step 2 $\mathbf{D}_{k+1} = \mathbf{D}_k \cup \{(\mathbf{x}_f^i, \hat{\theta}_{k+1})\}_{1 \leq i \leq n}$.

Step 3 Run the code over all new locations $\{(\mathbf{x}_f^i, \hat{\theta}_{k+1})\}_{1 \leq i \leq n}$.

Step 4 Update the Gaussian process distribution based on $y(\mathbf{D}_{k+1})$.

Step 5 Let $m_{k+1} := \min \{m_0, \dots, m_k, SS(\hat{\theta}_{k+1})\}$.

Because the distribution of the GPE is updated at Step 4, the hyper-parameters β , σ^2 and Ψ are re-estimated, as done in the seminal EGO work (Jones et al., 1998). Algorithm 1 could be efficiently performed by running the new simulations at Step 3 simultaneously on several

computer nodes. We present below the steps of a one-at-a-time algorithm well-suited when the computer system has a single processor.

Algorithm 2

Initialization is similar to Algorithm 1 except that $\mathbf{D}_1 = \mathbf{D}_0 \cup \{(\mathbf{x}^*, \hat{\boldsymbol{\theta}}_1)\}$.

For $k = 1, \dots, N - N_0$, repeat the same steps as in Algorithm 1 except that Step 3 is replaced with Step $\tilde{3}$ and Step 5 is replaced with Step $\tilde{5}$.

Step $\tilde{3}$ Run the code in $(\mathbf{x}^*, \hat{\boldsymbol{\theta}}_{k+1})$ where $\mathbf{x}^* = \underset{\mathbf{x}_f^i \in \mathbf{X}_f}{\operatorname{argmax}} \operatorname{Crit}(\mathbf{x}_f^i, \hat{\boldsymbol{\theta}}_{k+1})$ (see Equations (27) and (29) below).

Step $\tilde{5}$ $m_{k+1} := \min \{\mathbb{E}[SS^k(\hat{\boldsymbol{\theta}}_1)], \dots, \mathbb{E}[SS^k(\hat{\boldsymbol{\theta}}_k)], \mathbb{E}[SS^k(\hat{\boldsymbol{\theta}}_{k+1})]\}$

Algorithm 2 should be understood as an approximation of Algorithm 1 where only a single simulation $y_{\hat{\boldsymbol{\theta}}_{k+1}}(\mathbf{x}^*)$ is run at each iteration. In the following, two criteria are proposed to pick up \mathbf{x}^* among \mathbf{X}_f . As the current minimum m_k in Algorithm 1 can not be computed anymore, we have replaced it with the minimum of the expectations $\mathbb{E}[SS^k(\hat{\boldsymbol{\theta}}_i)]$ for $1 \leq i \leq k+1$ with respect to $Y^k(\cdot)$.

The first criterion is done to run the code at the input location $(\mathbf{x}^*, \hat{\boldsymbol{\theta}}_k) \in \mathbf{X}_f \times \mathcal{T}$ where the variance of $Y^k(\cdot)$ is at the highest. Hence,

$$\operatorname{Crit}(\mathbf{x}_f^i, \hat{\boldsymbol{\theta}}_{k+1}) = \mathbb{V}[Y^k(\mathbf{x}_f^i, \hat{\boldsymbol{\theta}}_{k+1})]. \quad (27)$$

As the variance of the Gaussian process decreases on the space $\mathbf{X}_f \times \mathcal{T}$, the approximated posterior distribution (18) comes close to the target posterior distribution (7), which justifies (27). Yet, a better way might perhaps consist in aiming for a reduction of the GPE uncertainty at an input location $(\mathbf{x}^*, \hat{\boldsymbol{\theta}}_{k+1})$ where the code $y_{\boldsymbol{\theta}}(\mathbf{x}^*)$ is highly variable over $\boldsymbol{\theta}$, meaning that \mathbf{x}^* is important for calibration. We thus introduce a second criterion which does a trade-off between the calibration goal and (27). A normalized version of it is written as

$$\operatorname{Crit}(\mathbf{x}_f^i, \hat{\boldsymbol{\theta}}_{k+1}) = \frac{\mathbb{V}(Y^k(\mathbf{x}_f^i, \hat{\boldsymbol{\theta}}_{k+1}))}{\max_{i=1, \dots, n} \mathbb{V}(Y^k(\mathbf{x}_f^i, \hat{\boldsymbol{\theta}}_{k+1}))} \times \frac{\mathbb{V}[y_{\boldsymbol{\theta}}(\mathbf{x}_f^i)]}{\max_{i=1, \dots, n} \mathbb{V}[y_{\boldsymbol{\theta}}(\mathbf{x}_f^i)]}, \quad (28)$$

where $\mathbb{V}[y_{\boldsymbol{\theta}}(\mathbf{x}_f^i)]$ is taken with respect to $\Pi(\boldsymbol{\theta})$. Since the code is unknown, an approximation of (28) can be based on the mean of $Y^k(\cdot)$:

$$\operatorname{Crit}(\mathbf{x}_f^i, \hat{\boldsymbol{\theta}}_{k+1}) = \frac{\mathbb{V}(Y^k(\mathbf{x}_f^i, \hat{\boldsymbol{\theta}}_{k+1}))}{\max_{i=1, \dots, n} \mathbb{V}(Y^k(\mathbf{x}_f^i, \hat{\boldsymbol{\theta}}_{k+1}))} \times \frac{\mathbb{V}[\mu_{\beta}^k(\mathbf{x}_f^i, \boldsymbol{\theta})]}{\max_{i=1, \dots, n} \mathbb{V}[\mu_{\beta}^k(\mathbf{x}_f^i, \boldsymbol{\theta})]}. \quad (29)$$

Remark 3. A typical problem inherent to sequential designs is when two input locations come very close, making the covariance matrix numerically singular and thus difficult to invert. This issue can arise when both $\hat{\boldsymbol{\theta}}_k$ is too close to a previous iteration $\hat{\boldsymbol{\theta}}_{k'}$ and \mathbf{x}^* is almost the same at iteration k , then at $k' > k$. The usual way to circumvent this issue consists in adding a small diagonal matrix to the covariance matrix $V_{\boldsymbol{\Psi}, \sigma^2}^{k'}(\boldsymbol{\theta})$ of the GPE, called nugget effect.

Remark 4. The expectation in (26) is taken with respect to the multivariate Gaussian distribution induced by the distribution of the GPE. Another way would have been to emulate the function $SS(\boldsymbol{\theta})$ as a Gaussian process, forcing n simulations to be run at each iteration. Doing so, one at a time algorithms would have been impossible, making this strategy irrelevant for large values of n .

Computation of the criterion By expanding Equation (26), we have :

$$EI^k(\boldsymbol{\theta}) = m_k \left[\mathbb{P}[SS^k(\boldsymbol{\theta}) < m_k] - \frac{\mathbb{E}[SS^k(\boldsymbol{\theta}) \mathbf{1}_{SS^k(\boldsymbol{\theta}) \leq m_k}]}{m_k} \right] > 0, \quad (30)$$

implying

$$\mathbb{E}[SS^k(\boldsymbol{\theta}) \mathbf{1}_{SS^k(\boldsymbol{\theta}) \leq m_k}] \leq m_k \mathbb{P}[SS^k(\boldsymbol{\theta}) < m_k]. \quad (31)$$

Except in the trivial case $n = 1$, no closed form can be calculated for (30). The expression of $EI^k(\boldsymbol{\theta})$ is proportional to the sum of $\mathbb{P}[SS^k(\boldsymbol{\theta}) < m_k]$ which is the probability of sampling inside the hypersphere $B(0, \sqrt{m_k})$ from a multivariate Gaussian distribution and a second term which is the expectation of the right truncated $SS^k(\boldsymbol{\theta})$ with respect to m_k . The first term can be calculated either as an infinite series in central chi-square distribution (Sheil and Muirheartaigh, 1977) or thanks to an advanced sampling rejection method (Ellis and Maitra, 2007). This second method should be preferably performed because the second term has to be estimated using MCMC. The minimization of (30) can be performed in a greedy fashion where $\hat{\boldsymbol{\theta}}_{k+1}$ is taken as the value which maximizes $EI^k(\boldsymbol{\theta})$ over a grid $G \in \mathcal{T}$. However, the computation of $EI^k(\boldsymbol{\theta})$ could be avoided for some candidates of G , as explained hereafter.

Computation of $\hat{\boldsymbol{\theta}}_{k+1}$

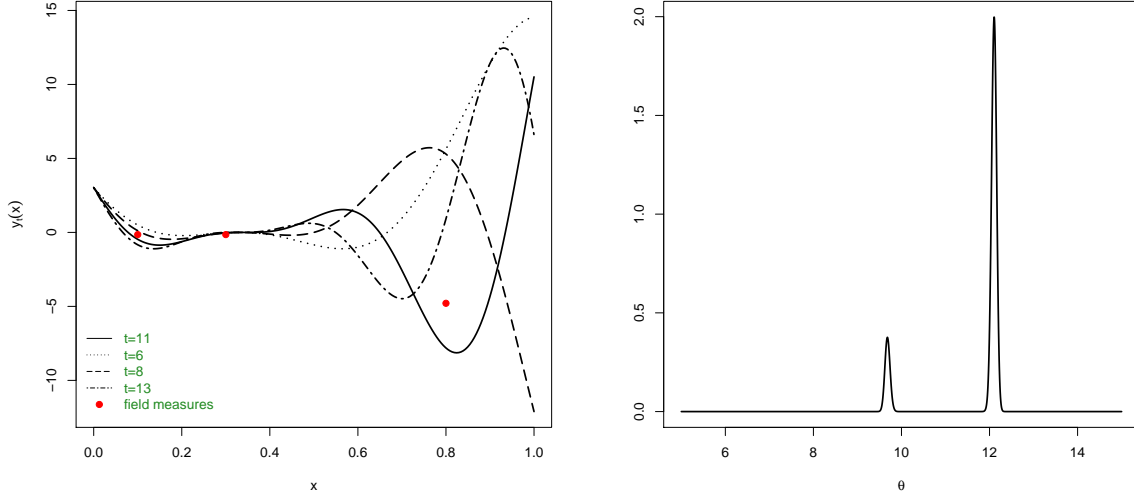
1. Compute $\mathbb{P}[\mathbf{z}_f - Y_{\boldsymbol{\theta}}^k \in [-m_k, m_k]^n]$ which is an upper bound of $\mathbb{P}[SS^k(\boldsymbol{\theta}) \leq m_k]$ for each $\boldsymbol{\theta}$ of G ,
2. Let $\tilde{\boldsymbol{\theta}} = \underset{\boldsymbol{\theta} \in G}{\operatorname{argmax}} \mathbb{P}[\mathbf{z}_f - Y_{\boldsymbol{\theta}}^k \in [-m_k, m_k]^n]$ be a reference value.
3. Compute $EI^k(\tilde{\boldsymbol{\theta}})$,
4. Build the sub-grid $\tilde{G} = \{\boldsymbol{\theta} \in \mathcal{T} ; EI^k(\tilde{\boldsymbol{\theta}}) \leq \mathbb{P}[\mathbf{z}_f - Y_{\boldsymbol{\theta}}^k \in [-m_k, m_k]^n]\} \subset G$,
5. Compute $EI^k(\boldsymbol{\theta})$ for the values of the sub-grid \tilde{G} ,
6. Let $\hat{\boldsymbol{\theta}} = \underset{\boldsymbol{\theta} \in \tilde{G}}{\operatorname{argmax}} EI^k(\boldsymbol{\theta})$.

For $\boldsymbol{\theta} \in G \setminus \tilde{G}$, we have $EI^k(\tilde{\boldsymbol{\theta}}) \geq \mathbb{P}[\mathbf{z}_f - Y_{\boldsymbol{\theta}}^k \in [-m_k, m_k]^n]$ implying $EI^k(\tilde{\boldsymbol{\theta}}) > EI^k(\boldsymbol{\theta})$. Hence, there is no need to compute $EI^k(\boldsymbol{\theta})$. Unfortunately, this algorithm is only relevant when n is small because in higher dimensions, the hypercube $[-m_k, m_k]^n$ has a much larger volume than the hypersphere.

Such a greedy optimization works very well on our toy examples, especially in small dimensions of \mathcal{T} because G can be constructed fine enough (see Section 4). In higher dimensions, the EI criterion could be maximized alternatively over several different grids as iterations of the EGO algorithm (see Section 4). However, if G is coarser, we can expect our algorithms stay efficient in terms of reducing the KL-divergence because they do not aim at converging precisely to the global minimum of $SS(\boldsymbol{\theta})$, but rather identifying the area of the input space where $SS(\boldsymbol{\theta})$ is small.

4 Simulations

Figure 1: *Left: the function $y_t(x) = (6x - 2)^2 \times \sin(tx - 4)$ on $[0, 1]$ for several values of $t \in [5, 15]$. Red dots are the field measurements $(\mathbf{X}_f, \mathbf{z}_f)$ generated by Equation (33). Right: the target posterior distribution.*



A 2D example Let us assume that the computer code is given by the following function:

$$y_t : x \longrightarrow y_t(x) = (6x - 2)^2 \times \sin(tx - 4), \quad (32)$$

where $x \in \mathcal{X} = [0, 1]$ and $t \in \mathcal{T} = [5, 15]$. For $1 \leq i \leq n$, the field data \mathbf{z}_f are generated by

$$z_f^i = y_\theta(x_f^i) + \epsilon^i, \quad (33)$$

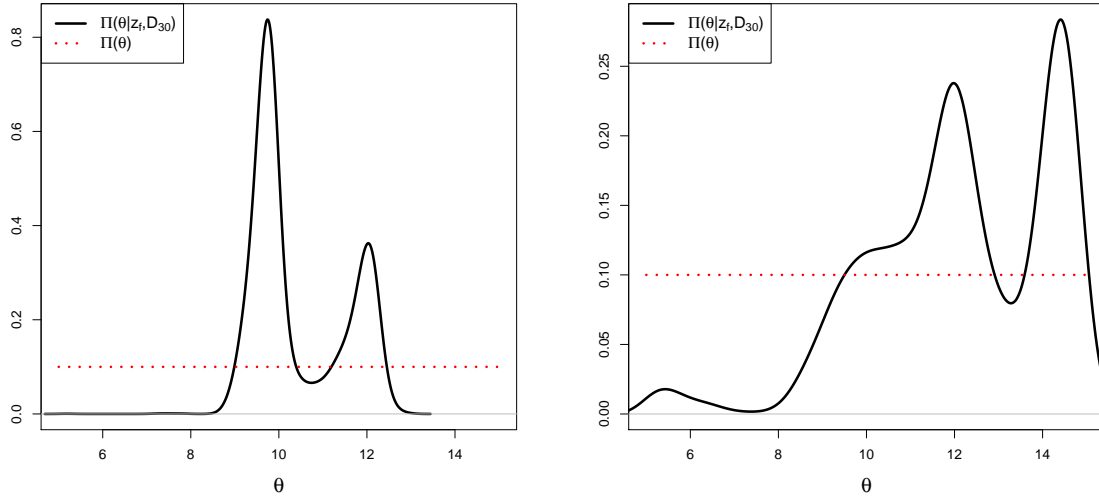
where $\theta = 12$ and $\epsilon_i \sim \mathcal{N}(0, 0.3^2)$. Bayesian calibration of the function (32) is done by sampling the target posterior distribution (7) (see Figure 1) where the prior distribution $\Pi(\theta)$ is chosen as uniform on $[5, 15]$:

$$\Pi(\theta) \propto \mathbf{1}_{[5, 15]}. \quad (34)$$

Now, Bayesian calibration of (32) is done by sampling the approximated posterior distribution (18). Two cases are considered: with $n = 3$ field measurements, then with $n = 9$ field measurements.

Case 1: $\mathbf{X}_f = (0.1, 0.3, 0.8)$ The approximated posterior distribution (18) is sampled from a GPE with a constant mean $m_\beta = m$ and a Matern 5/2 correlation function. All the parameters m, σ^2, Ψ have been estimated under the modular approach based on a maximin LHD of size $N = 30$ constructed with the R library DiceDesign. This calibration procedure is repeated twice by sampling (18) from two different maximin LHD. According to the first one, as illustrated in Figure 2 (left), the regions of high posterior density corresponds to those of the target posterior distribution but the two modes are reversed in terms of height. According to the second one, as illustrated in Figure 2 (right), the posterior distribution is very erroneous. Such calibrations

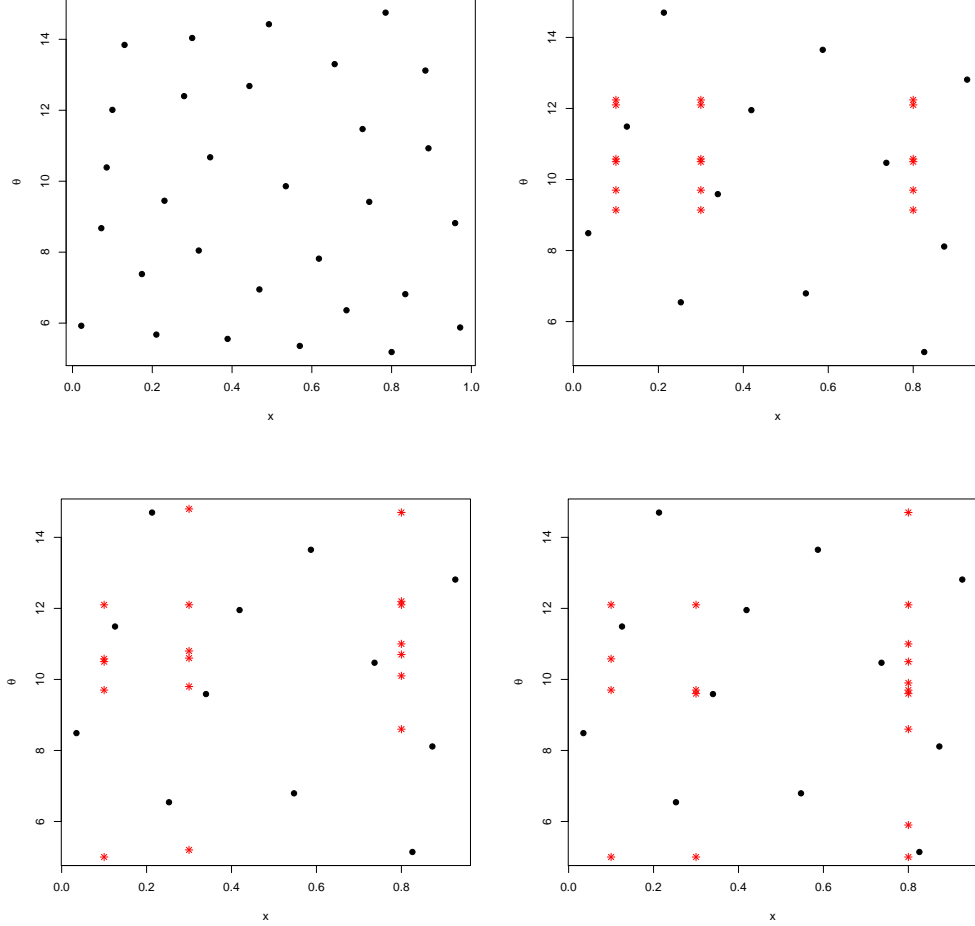
Figure 2: *Sampling of (18) from two different maximin LHD (using the R library MCMCpack).*



where the approximated posterior distribution is not close to the target one are unwanted, which justifies constructing some oriented designs for calibration instead of default space filling designs such as maximin LHD. In the following, three adaptive strategies building on the EGO algorithms from Section 3 are presented:

1. a first version based on Algorithm 1. At each iteration, the code is run at all three inputs $(0.1, \theta_k)$, $(0.3, \theta_k)$, $(0.8, \theta_k)$ where θ_k is the current parameter maximizing the EI criterion. An example of a design obtained with this algorithm is displayed in Figure 3 (upper right).
2. a second version based on Algorithm 2. The code is run at a single input (x^*, θ_k) where x^* comes from the input (x_i, θ_k) having the highest variance (27) among the three inputs $(0.1, \theta_k)$, $(0.3, \theta_k)$, $(0.8, \theta_k)$. An example of a design obtained with this algorithm is displayed in Figure 3 (bottom left).
3. a third version based on Algorithm 2. The code is run at a single input (x^*, θ_k) where x^* comes from the input (x_i, θ_k) which maximizes the criterion (29) among the three inputs $(0.1, \theta_k)$, $(0.3, \theta_k)$, $(0.8, \theta_k)$. An example of a design obtained with this algorithm is displayed in Figure 3 (bottom right)

Figure 3: *Case 1. Upper left: a maximin LHD ($N = 30$). Upper right: a sequential design built from Version 1 ($N_0 = 12$). Bottom left: a sequential design built from Version 2 ($N_0 = 12$). Bottom right: a sequential design built from Version 3 ($N_0 = 12$). The black dots are the initial design. The red stars are the new experiments selected from the EI criterion.*



Let us now assess how good is the calibration by computing $\text{KL}(\Pi(\theta|\mathbf{z}_f)||\Pi^C(\theta|\mathbf{z}_f, y(\mathbf{D}_N)))$ according to the kind of design \mathbf{D}_N which is used. The proportion of the time that the 95% credibility interval of (18) covers the true value is computed as well. The robustness of the results is checked by repeating sampling of the approximated posterior distribution (18) many times. Here, calibration is performed from 50 data sets $(\mathbf{X}_f, \mathbf{z}_f)$ and for each of them, 50 calibrations derived from 50 different designs have been conducted. In Figure 4, the boxplots of the KL divergence and the boxplots of the coverage are each plotted against the kind of design (including the maximin LHD and the sequential designs coming from the EGO algorithms). Each value of the boxplot is computed as the mean of the criterion over the 50 calibrations derived from a particular data set $(\mathbf{X}_f, \mathbf{z}_f)$. A sharp decrease in the KL divergence is noticed when the calibration is done with a sequential design. We can see that both versions 2 and 3 have the lowest values for this criterion. The reason is that Algorithm 2 can move more quickly inside the parameter space \mathcal{T} , which is expected when the target posterior distribution is multimodal. Results about coverage look the same although some lower values can be seen. In such cases,

the coverage is poor because the true value ($\theta = 12$) is not covered by the 95% interval of the target posterior distribution. The same feature is thus expected with the approximated posterior distribution.

Figure 4: *Case 1. Left: boxplots of the KL divergence computed between the target posterior distribution and the approximated posterior distribution (using the R library FNN). Right: ability of the 95% credibility interval to cover the true value ($\theta = 12$).*

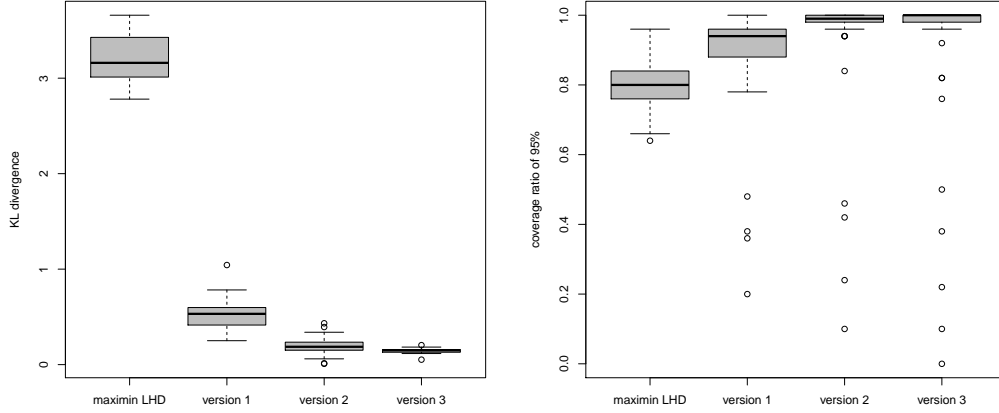
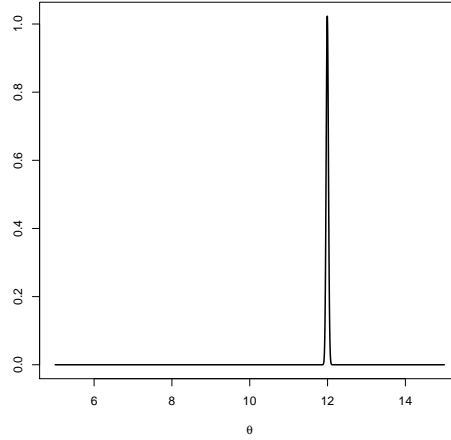


Figure 5: *The target posterior distribution (Case 2)*

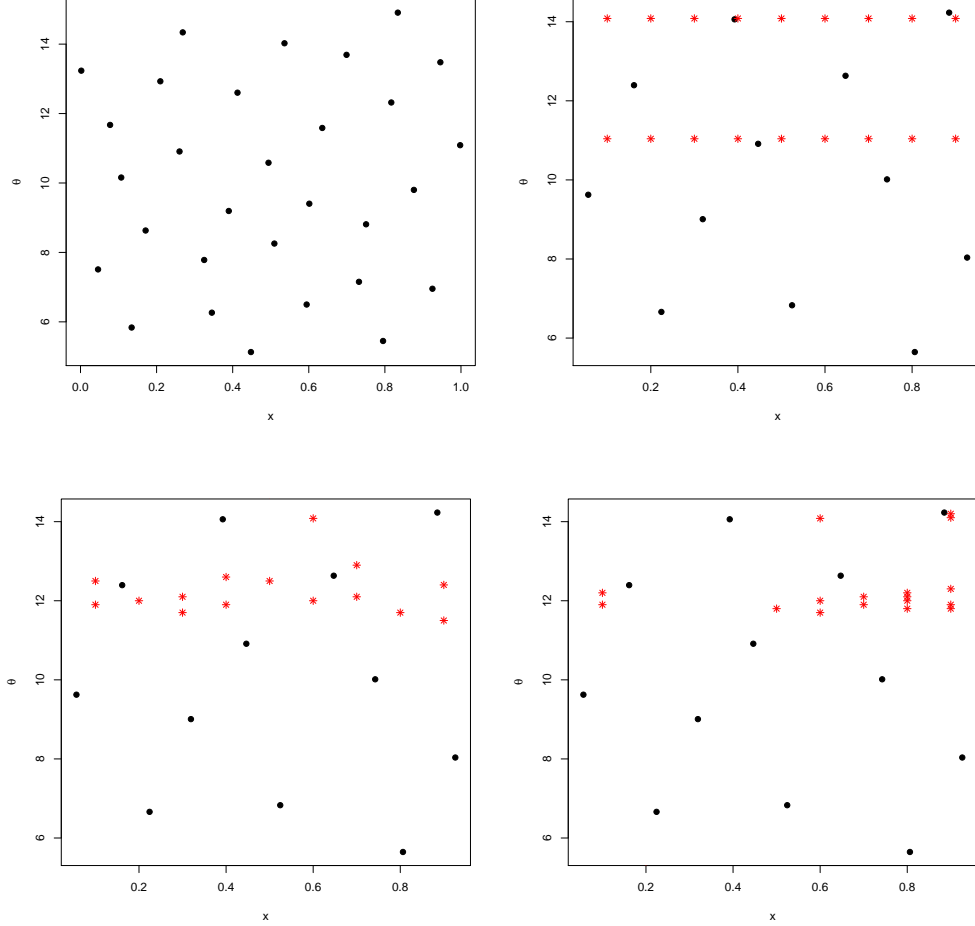


Case 2: $\mathbf{X}_f = (0.1, 0.2, 0.3, 0.4, 0.5, 0.6, 0.7, 0.8, 0.9)$ The field data \mathbf{z}_f are still generated by

$$z_f^i = y_\theta(x_f^i) + \epsilon^i \quad \text{for } i = 1, \dots, n, \quad (35)$$

where $\theta = 12$ and $\epsilon^i \sim \mathcal{N}(0, 0.3^2)$. As n is larger, the target posterior distribution $\Pi(\theta|\mathbf{z}_f)$ now has a single narrow mode around the true value. Similar to the first case, the calibration results are improved by using adaptive designs (see Figure 7). As the number of field data is larger, the one-at-a-time Versions 2 and 3 outperform Version 1 because they do not need all

Figure 6: *Case 2. Upper left: a maximin LHD ($N = 30$). Upper right: a sequential design built from Version 1 ($N_0 = 12$). Bottom left: a sequential design built from Version 2 ($N_0 = 12$). Bottom right: a sequential design built from Version 3 ($N_0 = 12$). The black dots are the initial design. The red stars are the new experiments selected from the EI criterion.*



the evaluations corresponding to a θ around 14 to discard this area, and evaluations remain to refine the sampling around $\theta = 12$ (see Figure 6).

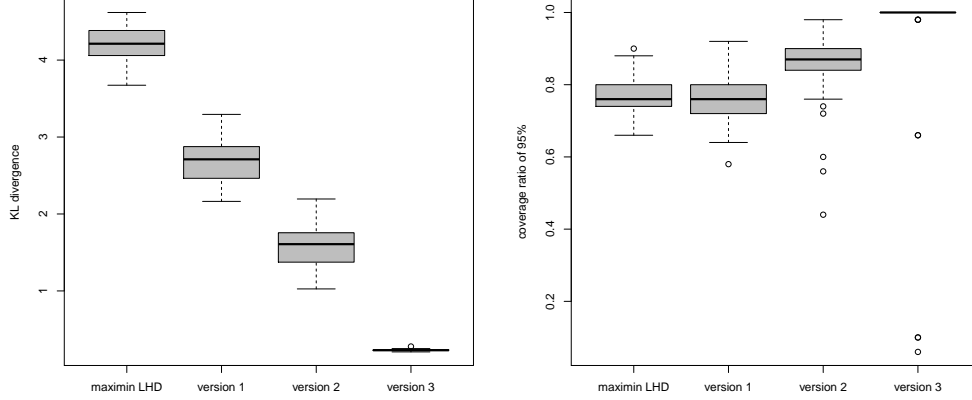
A 6D example Inspired from Saltelli et al. (2000), let us now assume that the computer code is given by the following function:

$$g_{\tau} : \mathbf{x} \longrightarrow g_{\tau}(\mathbf{x}) \prod_{i=1}^3 \frac{|4x_i - 2| + \tau_i}{1 + \tau_i}. \quad (36)$$

This highly non-linear function is used within the field of global sensitivity analysis to assess the efficiency of new methods (Marrel, 2008). For $1 \leq i \leq n = 60$, the field data \mathbf{z}_f are still generated by

$$z_f^i = g_{\theta}(x_f^i) + \epsilon^i, \quad (37)$$

Figure 7: *Case 2. Left: boxplots of the KL divergence computed between the target posterior distribution and the approximated posterior distribution (using the R library FNN). Right: ability of the 95% credibility interval to cover the true value ($\theta = 12$).*



where $\boldsymbol{\theta} = (0.34, 0.34, 0.34)$ and $\epsilon^i \sim \mathcal{N}(0, 0.05^2)$. Here, both \mathbf{x} and $\boldsymbol{\theta}$ are three-dimensional vectors. In the same spirit as before, we aim at reducing the calibration error between the unknown target posterior (7) and the approximated posterior (18). The prior distribution $\Pi(\boldsymbol{\theta})$ is chosen as uniform on $[0, 1]^3$:

$$\Pi(\boldsymbol{\theta}) \propto \mathbf{1}_{[0,1]^3}. \quad (38)$$

Let the allocated number of simulations be equal to $N = 200$. Similar to the 2D example, maximin LHD are compared with the sequential designs. Given the size of field data ($n = 60$), only Version 2 and Version 3 are performed, both starting from an initial design of size $N_0 = 100$ simulations. As explained in Section 3, a discretization G of the parameter space is required for maximizing the EI criterion. Given that the dimension of $\boldsymbol{\theta}$ is larger than in the previous example, the choice of such a grid is more sensitive. Indeed, if G is too coarse, some promising area of the parameter space could be not explored whereas if G is too fine, the computation time will be drastically increased. The solution that we suggest to address this problem consists in maximizing the EI criterion alternatively on several designs, as iterations, so that:

$$G = G_1 \cap G_2 \cap \dots \cap G_M \quad (39)$$

and

$$G_1 \cap G_2 \cap \dots \cap G_M = \emptyset. \quad (40)$$

In this example, for simplicity we have chosen $M = 2$ grids and,

$$G_1 = [0, 0.2, 0.4, 0.6, 0.8, 1] \times [0, 0.2, 0.4, 0.6, 0.8, 1] \times [0, 0.2, 0.4, 0.6, 0.8, 1]$$

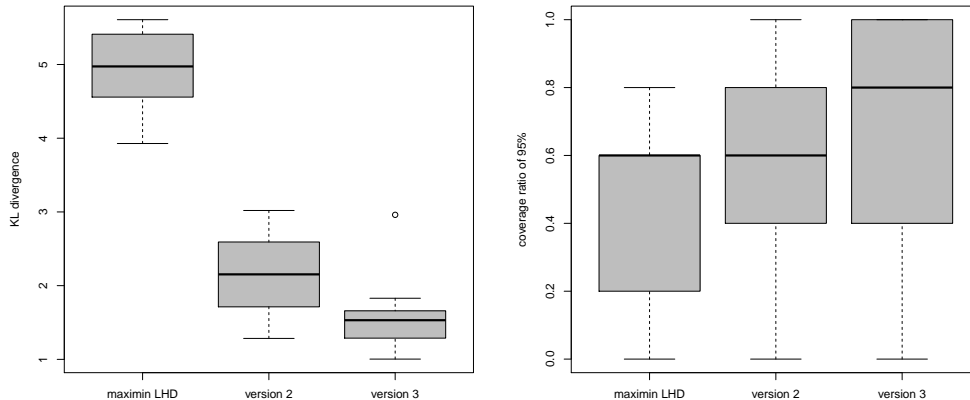
and

$$G_2 = [0.1, 0.3, 0.5, 0.7, 0.9] \times [0.1, 0.3, 0.5, 0.7, 0.9] \times [0.1, 0.3, 0.5, 0.7, 0.9].$$

Thus, for odd iterations the EI criterion is maximized over G_1 whereas for even iterations the EI criterion is maximized over G_2 . The calibration results are illustrated in Figure 8. They look the same as those of the 2D example, which again support the advantage of using a sequential design. Let us see that neither G_1 nor G_2 covers the unknown true value. One can think that a more

exhaustive decomposition in (39) would make G closer to the true value $\theta = (0.34, 0.34, 0.34)$, perhaps making the results even better. Boxplots for coverage rate have larger variance than in the previous examples because each of the 95% credibility interval of the three marginal posterior distribution needs to cover the true value 0.34.

Figure 8: *Left: boxplots of the KL divergence computed between the target posterior distribution and the approximated posterior distribution (using the R library FNN). Right: Coverage rate. For both figures, boxplots are made over 50 calibrations.*



5 Conclusions

This paper deals with new adaptive numerical designs for calibrating time-consuming computer codes in a Bayesian setting. For such codes, Bayesian calibration is based on a Gaussian process emulator (GPE) which approximates the code output and thus making the MCMC algorithms practicable. After choosing a design of experiments, the GPE is estimated by using a modular approach which allows us to separate the estimation of GPE parameters from the estimation of the code parameters.

Our contribution consists in taking advantage of the stochastic property of the GPE to build sequentially the design of experiments in such a way that the gap between the posterior distribution based on the GPE (the so-called approximated posterior distribution) and the posterior distribution based on the code (the so-called target posterior distribution) is the smallest possible in terms of the KL-divergence. We have shown it is of a great importance to reduce the uncertainty of the GPE where the density of the target posterior distribution is large. In an objective Bayesian context where no prior expertise is available about the unknown parameters, this goal is equivalent to reduce the uncertainty of the GPE where the sum of squares of the residuals between the code outputs and the field measurements is small. We have thus proposed sequential strategies for building the design of experiments based on the EI criterion designed for the sum of squares of the residuals. Our simulations on toy functions have shown such designs outperform space-filling designs in terms of low value of the KL-divergence. However, simulations have been performed in an unbiased framework where there is no discrepancy between the physical system and the computer code. If prior information is available about the shape of the code discrepancy, our algorithms could be applied to a weighted sum of squares function in a similar way.

It may appear surprising that the prior distribution is not taken into account in the EI maximization. That is because the prior distribution is identical both for the approximated posterior distribution and the target posterior distribution. Furthermore, if we aim at conducting a sensitivity analysis to the choice of the prior distribution, then we would like to be able to perform several calibrations from different prior distributions without having to rebuild a GPE each time.

The main difference between the algorithms presented in this paper and the current use of the EGO algorithm is that the objective function, that is the sum of squares of the residuals, is not modeled by a Gaussian process. Such modeling makes possible to conduct one-at-a-time sequential strategies where a single simulation $y_{\hat{\theta}_k}(\mathbf{x}^*)$ is run at each iteration. Two criteria have been suggested to pick up \mathbf{x}^* among the input field measurements but more sophisticated criteria might be more relevant. In addition, we might be also think about an EGO algorithm which would be designed according to the number of available computers nodes.

Another concern is how to maximize the EI criterion over the parameter space. Because it has no closed form expression, the optimization is performed in a greedy fashion, but free-derivative optimization algorithms could be also used (Conn et al., 2009).

Finally, our EGO algorithms start from a maximin LHD on $\mathcal{X} \times \mathcal{T}$ whereas the posterior distribution only depends on the simulations running in the space $\mathbf{X}_f \times \mathcal{T}$. A better strategy could be to build a space filling design on this input space.

6 Acknowledgments

The authors of the paper want to thank Joan Sobota for correcting English mistakes. This work was supported by the research contract CIFRE $n^\circ 456/2012$ between Électricité de France and AgroParisTech.

Appendix : Proof of Proposition 1

Proof. We refer to the log-conditional likelihood as $\ell^C(\mathbf{z}_f|\boldsymbol{\theta}, y(\mathbf{D}_N)) = \log(\mathcal{L}^C(\mathbf{z}_f|\boldsymbol{\theta}, y(\mathbf{D}_N)))$ and the target log-likelihood as $\ell(\mathbf{z}_f|\boldsymbol{\theta}) = \log(\mathcal{L}(\mathbf{z}_f|\boldsymbol{\theta}))$. It is sufficient to prove that

$$|\ell^C(\mathbf{z}_f|\boldsymbol{\theta}, y(\mathbf{D}_N)) - \ell(\mathbf{z}_f|\boldsymbol{\theta})| \quad (41)$$

is uniformly bounded in $\boldsymbol{\theta}$ and the bound tends to zero with $N \rightarrow \infty$. We can decompose (41) as

$$|\ell^C(\mathbf{z}_f|\boldsymbol{\theta}, y(\mathbf{D}_N)) - \ell(\mathbf{z}_f|\boldsymbol{\theta})| \leq |\ell^C(\mathbf{z}_f|\boldsymbol{\theta}, y(\mathbf{D}_N)) - \tilde{\ell}^C(\mathbf{z}_f|\boldsymbol{\theta}, y(\mathbf{D}_N))| + |\tilde{\ell}^C(\mathbf{z}_f|\boldsymbol{\theta}, y(\mathbf{D}_N)) - \ell(\mathbf{z}_f|\boldsymbol{\theta})| \quad (42)$$

where

$$\tilde{\ell}^C(\mathbf{z}_f|\boldsymbol{\theta}, y(\mathbf{D}_N)) = -\frac{1}{2\lambda^2}(\mathbf{z}_f - \mu_{\boldsymbol{\beta}}^N(\mathbf{X}_f, \boldsymbol{\theta}))^T(\mathbf{z}_f - \mu_{\boldsymbol{\beta}}^N(\mathbf{X}_f, \boldsymbol{\theta})) - \frac{n}{2} \log 2\pi - n \log \lambda$$

corresponds to the log-conditional likelihood where the function y is replaced with $\mu_{\boldsymbol{\beta}}^N$ and the covariance matrix of the GPE is neglected. The second term is bounded as:

$$\begin{aligned} |\tilde{\ell}^C(\mathbf{z}_f|\boldsymbol{\theta}, y(\mathbf{D}_N)) - \ell(\mathbf{z}_f|\boldsymbol{\theta})| &= \left| -\frac{1}{2\lambda^2} \left(\|\mathbf{z}_f - \mu_{\boldsymbol{\beta}}^N(\mathbf{X}_f, \boldsymbol{\theta})\|^2 - \|\mathbf{z}_f - y_{\boldsymbol{\theta}}(\mathbf{X}_f)\|^2 \right) \right| \\ &= \left| -\frac{1}{2\lambda^2} \left(\sum_{i=1}^n (y_{\boldsymbol{\theta}}(\mathbf{x}_f^i) - \mu_{\boldsymbol{\beta}}^N(\mathbf{x}_f^i, \boldsymbol{\theta})) (2z_f^i - y_{\boldsymbol{\theta}}(\mathbf{x}_f^i) - \mu_{\boldsymbol{\beta}}^N(\mathbf{x}_f^i, \boldsymbol{\theta})) \right) \right|. \end{aligned}$$

Let us suppose that the minimax distance, say $(h_{\mathbf{D}_N})_N$, of the designs sequence $(\mathbf{D}_N)_N$ tends to 0, namely

$$h_{\mathbf{D}_N} = \max_{(\mathbf{x}', \boldsymbol{\tau}') \in \mathcal{T} \times \mathcal{X}} \min_{(\mathbf{x}_i, \boldsymbol{\tau}_i) \in \mathbf{D}_N} \|(\mathbf{x}', \boldsymbol{\tau}') - (\mathbf{x}_i, \boldsymbol{\tau}_i)\| \xrightarrow{N \rightarrow \infty} 0 \quad (43)$$

Then, the uniform bound is deduced from the point-wise bound given for standard radial basis correlation function C_ψ (Schaback, 1995). We can obtain

$$|y_{\boldsymbol{\theta}}(\mathbf{x}_f^i) - \mu_{\boldsymbol{\beta}}^N(\mathbf{x}_f^i, \boldsymbol{\theta})| \leq \|y\|_{C_\psi} \cdot G_{C_\psi}(h_{\mathbf{D}_N}), \quad (44)$$

where $\|y\|_{C_\psi}$ is the norm of y in the RKHS associated to C_ψ and $G_{C_\psi}(\cdot)$ tends to 0 when $h_{\mathbf{D}_N}$ tends to 0.

We know that the distance is maximum when $\|\mathbf{z}_f - \mu_{\boldsymbol{\beta}}^N(\mathbf{X}_f, \boldsymbol{\theta})\| = 0$. Hence, the first term in (42) is written as,

$$\begin{aligned} |\ell^C(\mathbf{z}_f | \boldsymbol{\theta}, y(\mathbf{D}_N)) - \tilde{\ell}^C(\mathbf{z}_f | \boldsymbol{\theta}, y(\mathbf{D}_N))| &\leq \left| \frac{1}{2} \log(|V_{\boldsymbol{\Psi}, \sigma^2}^N(\boldsymbol{\theta}) + \lambda^2 \mathbf{I}_n|) - \frac{n}{2} \log(\lambda^2) \right| \\ &= \left| \frac{1}{2} \log \left(\frac{|V_{\boldsymbol{\Psi}, \sigma^2}^N(\boldsymbol{\theta}) + \lambda^2 \mathbf{I}_n|}{(\lambda^2)^n} \right) \right| \\ &\leq \left| \frac{1}{2} \log \left(\frac{\sum_{i=1}^n (V_{\boldsymbol{\Psi}, \sigma^2}^N(\boldsymbol{\theta})(i, i)/n) + \lambda^2}{\lambda^2} \right) \right| \\ &= \left| \frac{n}{2} \log \left(\frac{\sum_i V_{\boldsymbol{\Psi}, \sigma^2}^N(\boldsymbol{\theta})(i, i)}{\lambda^2 n} + 1 \right) \right| \end{aligned}$$

where the inequality of arithmetic and geometric means is used for bounding the determinant by a function of the trace. Using again results in Schaback (1995), we obtain $V_{\boldsymbol{\Psi}, \sigma^2}^N(\boldsymbol{\theta})_{ii} \leq G_{C_\psi}(h_{\mathbf{D}_N})$. Therefore,

$$|\ell^C(\mathbf{z}_f | \boldsymbol{\theta}, y(\mathbf{D}_N)) - \tilde{\ell}^C(\mathbf{z}_f | \boldsymbol{\theta}, y(\mathbf{D}_N))| \leq CST_y \cdot \frac{n}{\lambda^2} G_{C_\psi}(h_{\mathbf{D}_N}).$$

Since $(h_{\mathbf{D}_N})_N$ tends to 0 with N , putting the two bounds together proves the uniform convergence of (41) to 0. □

References

- Bachoc, F. (2014). Asymptotic analysis of the role of spatial sampling for covariance parameter estimation of Gaussian processes. *Journal of Multivariate Analysis*, 125:1–35.
- Bastos, L. and O’Hagan, A. (2008). Diagnostics for Gaussian process emulators. *Technometrics*, 51:425–438.
- Bayarri, M., Berger, J., Paulo, R., Sacks, J., Cafeo, J., Cavendish, J., Lin, C., and Tu, J. (2007). A framework for validation of computer models. *Technometrics*, 49:138–154.
- Box, G. E. P. and Tiao, G. T. (1973). *Bayesian Inference in Statistical Analysis*. Addison-Wesley, Reading.

- Brynjarsdottir, J. and O'Hagan, A. (2014). Learning about physical parameters: The importance of model discrepancy. Inverse Problems, 30:3251–3269.
- Campbell, K. (2006). Statistical calibration of computer simulations. Reliability Engineering and System Safety, 91:1358–1363.
- Conn, A., Sheinberg, K., and Vicente, L. (2009). Introduction to Derivative-Free Optimization. MOS SIAM Series on Optimization, Reading.
- Cover, T. and Thomas, J. (2006). Elements of Information Theory 2nd Edition. Wiley, New York.
- Cox, D., Park, J., and Clifford, E. (2001). A statistical method for tuning a computer code to a data base. Computational Statistics and Data Analysis, 37:77–92.
- Craig, P., Goldstein, M., Rougier, J., and Seheult, A. (2001). Bayesian forecasting for complex systems using computer simulators. Journal of the American Statistical Association, 96(454).
- Craig, P., Goldstein, M., Seheult, A., and Smith, J. (1997). Pressure Matching for Hydrocarbon Reservoir History: A Case Study in the Use of Bayes Linear Strategies for Large Computer Experiments, volume 121 of Lecture Notes In Statistics. Springer-Verlag.
- Currin, C., Mitchell, T., Morris, M., and Ylvisaker, D. (1991). Bayesian prediction of deterministic functions, with applications to the design and analysis of computer experiments. Journal of the Statistical Association, 86(416):953–963.
- Ellis, N. and Maitra, R. (2007). Multivariate Gaussian simulation outside arbitrary ellipsoids. Journal of Computational and Graphical Statistics, 16:692–708.
- Fang, K., Li, R., and Sudijanto, A. (2006). Design and modeling for computer experiments.
- Gang, H., Santner, T., and Rawlinson, J. (2009). Simultaneous determination of tuning and calibration parameters for computer experiments. Technometrics, 51:464–474.
- Ginsbourger, D. (2009). Multiplés Métamodèles pour l'approximation et l'optimisation de fonctions numériques multivariées. PhD thesis, Ecole Nationale Supérieure des Mines de Saint-Etienne.
- Gramacy, R., Bingham, D., Holloway, J., Grosskopf, M., Kuran, C., Rutter, E., Trantham, M., and Drake, P. (2014). Calibrating a large computer experiment simulating radiative shock hydrodynamics.
- Higdon, D., Kennedy, M., Cavendish, J., Cafo, J., and Ryne, R. (2004). Combining field data and computer simulations for calibration and prediction. SIAM Journal on Scientific Computing, 26:448–466.
- Janusevskis, J. and Le Riche, R. (2013). Simultaneous kriging-based estimation and optimization of mean response. Journal of Global Optimization, 55:313–336.
- Jones, D., Schonlau, M., and Welch, W. (1998). Efficient global optimization of expensive black-box functions. Journal of Global Optimization, 13:455–492.
- Joseph, V. and Melkote, S. (2009). Statistical adjustments to engineering models. Journal of Quality Technology, 41:362–375.

- Kass, R. and Wasserman, L. (1996). The selection of prior distributions by formal rules. Journal of the American Statistical Association, 91(435):1343–1370.
- Kennedy, M. and O’Hagan, A. (2001). Bayesian calibration of computer models (with discussion). Journal of the Royal Statistical Society, Series B, Methodological, 63:425–464.
- Koehler, J. and Owen, A. (1996). Computer experiments. Handbook of Statistics, Vol.13.
- Kumar, A. (2008). Sequential calibration of computer models. PhD thesis, The Ohio State University.
- Liu, F., Bayarri, M., and Berger, J. (2009). Modularization in bayesian analysis, with emphasis on analysis of computer models. Bayesian Analysis, 4(1):119–150.
- Loeppky, D., Bingham, D., and Welch, W. (2006). Computer model calibration or tuning in practice. Technical Report.
- Marrel, A. (2008). Mise en oeuvre et utilisation du méta-modèle processus gaussien pour l’analyse de sensibilité de modèles numériques. PhD thesis, CEA Cadarache.
- Pratola, M., Sain, S., Bingham, D., Wiltberger, M., and Rigler, E. (2013). Fast sequential computer model calibration of large nonstationary spatial-temporal processes. Technometrics, 55:232–242.
- Pronzato, L. and Muller, W. (2012). Design of computer experiments: space filling and beyond. Statistics and Computing, 22(3):681–701.
- Rasmussen, C. and Williams, C. (2006). Gaussian Processes for Machine Learning. the MIT press.
- Robert, C. and Casella, G. (1998). Monte Carlo Statistical Methods. Springer-Verlag.
- Roy, C. and Oberkampf, W. (2011). A comprehensive framework for verification, validation and uncertainty quantification in scientific computing. Computer Methods in Applied Mechanics and Engineering, 200:2131–2144.
- Sacks, J., Welch, W., Mitchell, T., and Wynn, H. (1989). Design and analysis of computer experiments. Technometrics, 31:41–47.
- Saltelli, A., Chan, K., and Scott, E. (2000). Sensitivity Analysis. Wiley, New York.
- Santner, T., Williams, B., and Notz, W. (2003). The Design and Analysis of Computer Experiments. Springer-Verlag.
- Schaback, R. (1995). Error estimates and condition numbers for radial basis function interpolation. Advances in Computational Mathematics, 3:251–264.
- Sheil, J. and Muirheartaigh, I. (1977). The distribution of non-negative quadratic forms in normal variables. Journal of the Royal Statistical Society, 26:92–98.
- Stein, M. (1999). Interpolation of Spatial Data: Some Theory for Kriging. Springer.
- Vazquez, E. and Bect, J. (2010). Convergence properties of the expected improvement algorithm with fixed mean and covariance functions. Journal of Statistical Planning and Inference, 140:3088–3095.

Wong, R., Storlie, C., and Lee, T. (2014). A frequentist approach to computer model calibration. Technical report, Iowa State University.